di(isononyl)cyclohexane-1,2-dicarboxylate (DINCH), an alternative for phthalate plasticizers. J Expo Sci Environ Epidemiol 2012;22: 201–211.
14. Nair CS, Vidya R, Ashalatha PM. Hexamoll DINCH plasticised PVC containers for the storage of platelets. Asian J Transfus Sci 2011; 5:18–22.
15. Jayakrishnan A, Sunny MC, Rajan MN. Photocrosslinking of azidated poly(vinyl chloride) coated onto plasticized PVC surface – Route to containing plasticizer migration. J Appl Poly Sci 1995;56: 1187–1195.
16. Miyamoto M, Sasakawa S. Effects of plasticizers and plastic bags on granulocyte function during storage. Vox Sang 1987;53:19–22.
17. Krishnan VK, Jayakrishnan A. Radiation grafting of hydrophilic monomers on to plasticized poly(vinyl chloride) sheets II. Migration behaviors of the plasticizer from N-vinyl pyrrolidone grafted sheets. Biomaterials 1991;12:489–492.
18. Ito R, Seshimo F, Haishima Y, Hasegawa C, Isama K, Yagami T, Nakahashi K, Yamazaki H, Inoue K, Yoshimura Y, Saito K, Tsuchiya T, Nakazawa H. Novel approach for reducing migration of di-2-ethylhexyl phthalate from polyvinyl chloride medical device. Int J Pharm 2005;303:104–112.
19. Haishima Y, Seshimo F, Higuchi T, Yamazaki H, Hasegawa C, Izumi S, Makino T, Nakahashi K, Ito R, Inoue K, Yoshimura Y, Saito K, Yagami T, Tsuchiya T, Nakazawa H. Development of a simple method for predicting the levels of di(2-ethylhexyl)phthalate migrated from PVC medical devices into pharmaceutical solutions. Int J Pharm 2005;298:126–142.
20. Haishima Y, Matsuda R, Hayashi Y, Hasegawa C, Yagami T, Tsuchiya T. Risk assessment of di(2-ethylhexyl) phthalate eluted from PVC blood circuits during hemodialysis and pump-oxygenation therapy. Int J Pharm 2004;274:119–129.
21. Hayashi Y, Matsuda R, Haishima Y, Yagami T, Nakamura, A. Validation of HPLC and GC-MS systems for bisphenol-A leached from hemodialyzers on the basis of FUMI theory. J Pharm Biomed Anal 2002;28:421–429.
22. Isama K, Matsuoka A, Haishima Y, Tsuchiya T. Proliferation and differentiation of normal human osteoblasts on dental Au-Ag-Pd casting alloy: Comparison with cytotoxicity to fibroblast L929 and V79 cells. Mater Transact 2002;43:3155–3159.
23. Matsuoka A, Onfelt A, Matsuda Y, Nakaoka R, Haishima Y, Yudasaka M, Iijima S, Tsuchiya T. 2009, Development of an in vitro screening method for safety evaluation of nanomaterials. Bio-Med Mater Eng 2009;19:19–27.
24. Matsuoka A, Sofuni T, Miyata N, Ishidate M Jr. Clastogenicity of 1-nitropyrene, fluorine, and mononitrofluorenes in cultured Chinese hamster cells. Mutat Res 1991;259:103–110.
25. Chen CY. The oxidation of di-(2-Ethylhexyl) phthalate (DEHP) in aqueous solution by UV/H_2O_2 photolysis. Water Air Soil Pollut 2010;209:411–417.
26. Ito R, Miura N, Ushiro M, Kawaguchi M, Nakamura H, Iguchi H, Ogino J, Oishi M, Wakui N, Iwasaki Y, Saito K, Nakazawa H. Effect of gamma-ray irradiation on degradation of di(2-ethylhexyl)phthalate in polyvinyl chloride sheet. Int J Pharm 2009;376:213–218.

Genes and Environment, Vol. 33, No. 1 pp. 14–20 (2011)

Review

In Vitro and *In Vivo* Genotoxicity Induced by Fullerene (C_{60}) and Kaolin

Yukari Totsuka[1,5], Tatsuya Kato[1,2], Shu-ichi Masuda[2], Kousuke Ishino[1], Yoko Matsumoto[1,3], Sumio Goto[3], Masanobu Kawanishi[4], Takashi Yagi[4] and Keiji Wakabayashi[2]

[1]Division of Cancer Development System, National Cancer Center Research Institute, Tokyo, Japan
[2]Department of Food & Nutritional Science, Graduate School of Nutrition & Environmental Science, University of Shizuoka, Shizuoka, Japan
[3]Laboratory of Environmental Risk Evaluation, School of Life and Enviromental Science, Azabu University, Kanagawa, Japan
[4]Environmental Genetics Laboratory, Frontier Science Innovation Center, Osaka Prefecture University, Osaka, Japan

(Received December 11, 2010; Revised December 22, 2010; Accepted December 26, 2010)

Nanomaterials are being utilized for many kinds of industrial products, and the assessment of genotoxicity and safety of nanomaterials is therefore of concern. In the present study, we examined the genotoxic effects of fullerene (C_{60}) and kaolin using *in vitro* and *in vivo* genotoxicity systems. Both nanomaterials significantly induced micronuclei and enhanced frequency of sister chromatid exchange (SCE) in cultured mammalian cells. When ICR mice were intratracheally instilled with these nanomaterials, DNA damage of the lungs increased significantly that of the vehicle control. Formation of DNA adducts in the lungs of mice exposed to nanomaterials were also analyzed by stable isotope dilution LC-MS/MS. 8-Oxodeoxyguanosine and other lipid peroxide related adducts were increased by 2- to 5-fold in the nanomaterial-exposed mice. Moreover, multiple (four consecutive doses of 0.2 mg per animal per week) instillations of C_{60} or kaolin, increased *gpt* mutant frequencies in the lungs of *gpt* delta transgenic mice. As the result of mutation spectrum analysis, G:C to C:G transversions were commonly increased in the lungs of mice exposed to both nanomaterials. In addition, G:C to A:T was increased in kaolin-exposed mice. In immunohistochemical analysis, many regions of the lungs that stained positively for nitrotyrosine (NT) were observed in mice exposed to nanomaterials. From these observations, it is suggested that oxidative stress and inflammatory responses are probably involved in the genotoxicity induced by C_{60} and kaolin.

Key words: nanomaterials, genotoxicity, fullerene (C_{60}), kaolin, DNA adducts

Introduction

Recently, nanomaterials are being utilized for cosmetics and industrial products, and applications in medicine are under consideration. The assessment of genotoxicity and safety of nanomaterials is therefore of concern. One reason behind this is the asbestos crisis (1). Some nanomaterials are not only nano-sized particles, but also asbestos shape-like fibers, and the carcinogenic potential of such nanomaterials has attracted much attention over the years. Moreover, it is thought that nano-sized particles can be taken up in cells and cause intracellular damage (2,3). With this background, we here investigated induction of *in vitro* and *in vivo* genotoxicity using fullerene (C_{60}) and kaolin as examples. To clarify the mechanisms of mutations due to these nanomaterials, we analyzed the formation of DNA adducts in the lungs of mice after exposure. Here, we briefly summarize our data and also discuss mechanisms of genotoxicity induced by nanomaterials.

Size Distribution in Suspensions of Nanomaterials

The size distribution of nanomaterials used in the present study was analyzed by dynamic light scattering (DLS) as described previously (4). The most abundant sizes were at 234.1 ± 48.9 and 856.5 ± 119.2 nm for C_{60} and 357.6 ± 199.4 nm for kaolin, respectively.

In Vitro Genotoxicity Test

Micronucleus test: The micronucleus genotoxicity/clastogenicity test is widely used for assessment of environmental substances and medicinal chemicals. Here, we investigated the micronucleus inducing activity of C_{60} and kaolin using human lung carcinoma A549

[5]Correspondence to: Yukari Totsuka, Division of Cancer Development System, National Cancer Center Research Institute, 1-1 Tsukiji 5 Chome, Chuo-ku, Tokyo 104-0045, Japan. Tel: +81-3-3542-2511, Fax: +81-3-3543-9305, E-mail: ytotsuka@ncc.go.jp

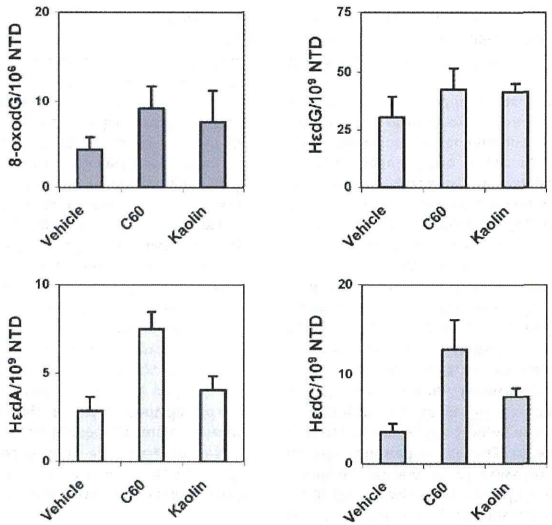

Fig. 4. Oxidative and lipid peroxide related DNA adduct formation in the lungs of ICR mice induced by nanoparticle exposure. DNA was extracted from lungs of mice 24 h after intratracheal instillation of 0.2 mg/body of C60 or kaolin, and digested enzymatically. Control animals were exposed to saline containing 0.05% Tween80. The 8-oxodG and 3 kinds of Hε-adducts were quantified by the stable isotope dilution LC-MS/MS method described by Chou *et al.* (10).

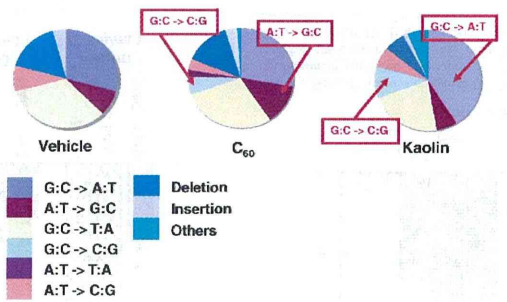

Fig. 5. Classification of *gpt* mutations from the lungs of control and nanoparticle treated mice.

tics induced by particles by PCR and DNA sequencing analysis of 6-TG resistant mutants. Classes of mutations found in the *gpt* gene are shown in Fig. 5. Interestingly, G:C to C:G transversions were increased in common with both particle treatments. Since these mutations were commonly increased regardless of the constituents (i.e., C_{60} is graphite and kaolin is aluminum silicate), the mechanisms might be the same. It has been reported that various oxidative stresses caused by sunlight, UV radiation, hydrogen peroxide and peroxy radicals frequently induce G:C to C:G transversions in various *in vitro* assay systems (14–17). Moreover, a variety of oxidative lesion products of guanine other than 8-oxodG, including imidazolone (Iz), oxazolone (Oz), spiroiminodihydantoin (Sp) and guanidinohydantoin (Gh), have been reported (18–24). Three such molecules, Oz, Sp and Gh are now thought to be key causes G to C transversions with translesion synthesis systems (22–25). Therefore, it is suggested that G:C to C:G transversions induced by C_{60} and kaolin could involve Oz, Sp and Gh formation. In addition, G:C to A:T transitions were also significantly increased by instillation of kaolin but not C_{60}. In general, G to A (or C to T) transitions have commonly been observed in spontaneous and chemically-induced mutants, and deamination of guanine or 5-methylcytosine might be involved. Burney *et al.* reported that nitric oxide induces DNA damage. NO can form N_2O_3, and direct by this agent can lead to DNA deamination via diazonium ion formation (26). Moreover, nitric oxide is produced by activated macrophages in inflamed organs. In fact, test substance-phagocytized macrophages and granulomas were frequently observed in the lungs of mice (4).

Immunohistochemical Analysis of Inflammation Factors

In order to confirm enhancement of nitric oxide production by C_{60} and kaolin, we examined immunohistochemical staining of an inflammation factor, nitrotyrosine (NT), in the lungs of *gpt* delta mice treated with these nanoparticles using the same procedure reported previously (27) with minor modification. As shown in Fig. 6, the pattern of NT staining corresponded to the areas of inflammation within lung parenchyma. In the case of C_{60} exposure, many regions of the lungs stained positively (data not shown), and intense NT staining was localized in test substance-phagocytized macrophages and granulomas. Similarly, staining with NT antibodies was observed in macrophages and alveolar epithelial cells in the lungs of mice exposed to kaolin, although to a lesser extent as compared with C_{60}.

Conclusion

Our results clearly demonstrated that both *in vitro* and *in vivo* genotoxicity are induced by C_{60} and kaolin. However, the mechanisms have yet to be fully clarified, and oxidative stress might be at least partly involved. There are a number of ways in which reactive oxygen species (ROS) could be generated: i) nanoparticles might trigger ROS production by iron-catalysed Fenton reactions; ii) nanoparticles could accumulate in cells due to phagocytosis, then enhance the production of ROS by NADPH oxidase (28,29). Recently, innate immune activation through Nalp3 inflammasomes has been suggested to play an important role in pulmonary fibrotic disorders of silicosis and asbestosis (30,31). It has been reported that proinflammatory cytokines, such as interleukin 1β are key molecules for pneumoconiosis. At

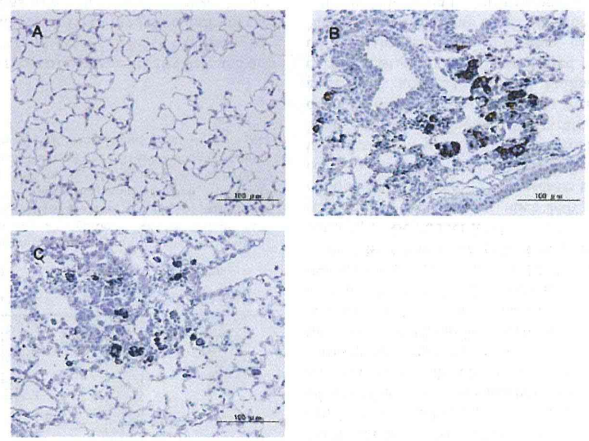

Fig. 6. Immunohistochemical localization of nitrotyrosine (NT). Since C_{60} is brown in color, we used an SG substrate kit (Vector Laboratories, USA) for peroxidase, with positive cells stained dark blue-gray. A: alveolar region in a control mouse, with no significant staining for NT. B: alveolar region in a mouse exposed to C_{60}, with positive macrophages phagocytizing test substance and epithelial cells. The brown colored material is C_{60}. C: alveolar region in a mouse exposed to kaolin. Note intense staining for NT in the granulomatous region.

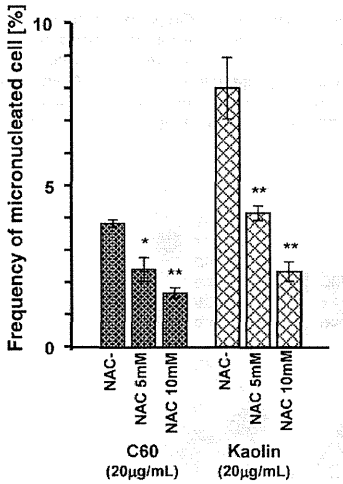

Fig. 1. Effects of anti-oxidative agents on the micronucleus inducing activity of nanoparticles. Values represent the means of three experiments ± SD. Asterisks (*, ** for $p<0.05$ and $p<0.01$, respectively) indicate significant differences from cells without NAC in the Student's t-test. Concentrations of nanoparticles in $\mu g/cm^2$ are given in parentheses.

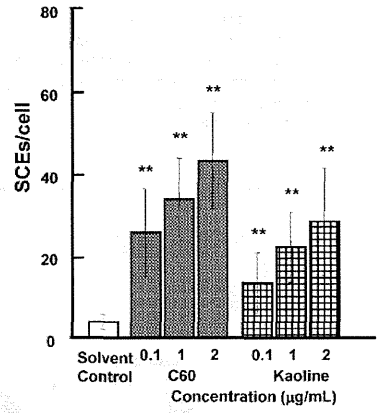

Fig. 2. Sister chromatid exchange (SCE) in CHO AA8 cells following treatment with C60 or kaolin for 1 h. The values represent the means of three experiments ± SD. Asterisks (**) indicate a significant difference ($p<0.01$) from control (treatment with 0.005% (v/v) Tween-80) cells in the Student's t-test.

cells (4). Six-hours treatment with 200 μg/mL kaolin caused growth inhibition of 60% whereas, C_{60} at the same concentration was without effect. C_{60} and kaolin particles both increased the number of micronucleated cells. The background frequency of micronucleated cells was 0.7% to 1.0%, and this rose to 10% and 5% with 200 μg/mL of C_{60} and kaolin, respectively, the increase being statistically significant in both cases. To investigate the effects of an anti-oxidative agent on the micronucleus induction, we conducted tests with or without *N*-acetyl cysteine (NAC) using Chinese hamster ovary CHO-AA8 cells. As shown in Fig. 1, the frequency of micronucleated cells was decreased significantly in the presence of NAC. With 20 μg/mL of C_{60} and kaolin for 6 h without NAC the results were 3.8% and 8%, respectively, but in the presence of 10 mM NAC these decreased to 1.7% and 2.3%. From this observation, oxidative stress might be involved in the genotoxicity induced by nanoparticles. Furthermore, it is known that photoexcited C_{60} produces reactive oxygen species (5) and in the present experiments, the cells and C_{60} were not shielded from visible light completely. Therefore, reactive oxygen species might contribute to micronucleus-induction in C_{60}-treated cells. On the other hand, biologically relevant features of kaolin are unclear and further studies will be required to elucidate genotoxic mechanisms.

Sister chromatid exchange (SCE) test: SCE is also used for mutagenic testing of many products. While the mechanisms responsible for SCE are not completely understood, they involve breakage of both DNA strands, followed by exchange of whole DNA duplexes. This occurs during the S phase and is efficiently induced by mutagens that form DNA adducts or that interfere with DNA replication. To investigate SCE inducing activity of nanoparticles, we examined CHO-AA8 cells following 1 h treatment with C_{60} and kaolin (Fig. 2). The SCE frequencies in cells treated with 2.0 μg/mL of C_{60} and kaolin were approximately 11 and 7 times higher than the control level, respectively ($P<0.01$ at 0.1 μg/mL or higher concentrations). C_{60} demonstrated stronger genotoxic/clastogenic potency than kaolin. Cozzi *et al.* earlier reported that H_2O_2-treatment produced reactive oxygen species and induced SCE in CHO cells, and antioxidants, such as ascorbic acid and β-carotene, reduced the frequency (6). In the present study, the results of the micronucleus test indicated involvement of reactive oxygen species so that they might contribute to SCE induction as well.

In Vivo Genotoxicity Test

Comet assay: The comet assay is known as a standard simple and sensitive technique for evaluation of

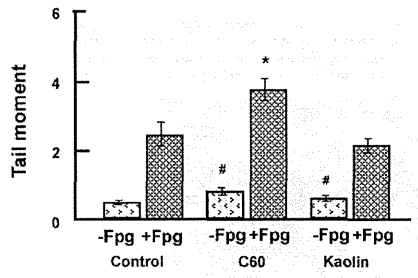

Fig. 3 DNA damage measured by comet assay in lungs of C57BL/6J mice intratracheally instilled with particles, with or without FPG treatment. Male mice were treated at a dose of 0.2 mg of particles per animal, and sacrificed 3 h after particle administration. The values represent the means of data for five animals ± SE. An asterisk (*) denotes $p<0.01$ from that of control (+FPG) and a sharp (♯) denotes $p<0.01$ from that of control (-FPG) in a Dunnett's test after one-way ANOVA of Tail Moment.

DNA damage. The types of damage usually detected are single and double strand breaks. The pH (usually between neutral and alkaline pH) of the lysis condition can be adjusted depending upon the type of damage. Under alkaline conditions, AP sites and others where excision repair takes place are detected as DNA damage. We here evaluated DNA damage induced by particles using the comet assay under alkaline conditions. The values for DNA tail moment in the lungs with single-particle treatment at 0.2 mg/body for 3 h were measured, and DNA damage was significantly increased, around 2-fold, as compared with the vehicle control, and its intensity was C_{60} > kaolin. When we examined the effects of oxidation of purines, DNA damage was analyzed by formamidopyrimidin-glycosilase (FPG)-modified comet assay. DNA damage induced by kaolin was not changed, whereas DNA damage caused by C_{60} was elevated up to 1.7 fold compared with the vehicle control (Fig. 3). In addition, Jacobsen *et al.* also reported that C_{60} significantly increased the level of FPG sensitive sites/oxidized purines determined by the comet assay using the E1-Mutatrade markMouse lung epithelial cell line (7). From these findings, it seems that oxidative damage would be partly involved in the induction of DNA damage by C_{60}, although other changes responsible for DNA damage might be induced by kaolin.

Oxidative and lipid peroxide related DNA adduct formation: DNA adducts, formed by reactions with exogenous or endogenous agents, are known to induce gene mutations. Reactive oxygen species (ROS) are one type of endogenous agent that can produce oxidative DNA adducts such as 8-oxo-2′-deoxyguanosine (8-oxodG), a widely recognized and utilized biomarker of oxidative stress, and a major mutagenic lesion producing predominately G to T transversion mutations (8). In addition, ROS generate lipid hydroperoxides to yield heptanon-etheno (Hε)-adducts, such as HεdG, HεdA and HεdC via 4-oxo-2-nonenal (4-ONE) (9). These adducts can lead to mutations, if not repaired. We examined whether these oxidative and lipid peroxide related DNA adducts were induced in the lungs of mice by intratracheally instilled nanomaterials. 8-OxodG and three kinds of Hε-adducts were analyzed in the lungs of ICR mice 3, 24, 72 and 168 h after intratracheal instillation of 0.2 mg/body of C_{60} or kaolin, and quantified by the stable isotope dilution LC-MS/MS method described by Chou *et al.* (10). Compared with a vehicle control, DNA adduct levels were increased by about 2- to 5-fold in the lungs of mice 24 h after injection of nanoparticles (Fig. 4). The increases were time dependent until 72 h then gradually decreased within 168 h of injection (data not shown). Related to this, oxidative DNA damage was induced by intratracheal instillation of C_{60} or kaolin in the comet assay with FPG treatment, as described above. In addition, Folkmann *et al.* reported that oral gavage of C_{60} increased the levels of 8-oxodG in the liver and the lungs of F344 rats (11). Moreover, Tsurudome *et al.* described increased 8-oxodG levels induced by intratracheally instilled diesel exhaust particles in the lungs of F344 rats, and 8-oxoguanine DNA glycosylase 1 (OGG1) mRNA was also overexpressed (12). The decreased DNA adducts in the present study at 168 h may have been a result of a repair enzyme such as OGG1. This is the first observation that Hε-lipid peroxide related DNA adducts are increased by nanoparticles. Such adducts could clearly contribute to nanomaterial-induced DNA damage and mutation. Our findings suggest involvement of ROS generation, although differences between C_{60} and kaolin still require clarification.

***gpt* Mutations in the lungs of *gpt* transgenic mice:** Transgenic *gpt* delta mice are a useful model system for detecting both point mutations and large deletions (< 10 kb) (13). λEG10 transgenes carrying gpt (detection of point mutations) and *red*, *gam* (detection of deletion) genes have been integrated into mouse chromosome 17, and point mutations and deletions observed in any tissues can be detected as 6-thioguanine (6-TG) resistant colonies and Spi^- plaques, respectively. To examine *in vivo* mutagenicity of nanoparticles, *gpt* delta transgenic mice were exposed to C_{60} and kaolin at four different doses by intratracheal instillation, and *gpt* mutations were analyzed. The background *gpt* mutant frequency (MF) in lungs was $10.3 \pm 0.53 \times 10^{-6}$. MFs were significantly increased by 2 to 3-fold to $30.75 \pm 3.32 \times 10^{-6}$ ($p=0.019$) for C_{60} and $19.30 \pm 4.82 \times 10^{-6}$ ($p=0.002$) for kaolin (4).

Moreover, we examined the mutational characteris-

Nanotoxicology, June 2013; 7(4):452–461
© 2013 Informa UK, Ltd.
ISSN: 1743-5390 print / 1743-5404 online
DOI: 10.3109/17435390.2012.674571

informa
healthcare

Genotoxicity of multi-walled carbon nanotubes in both *in vitro* and *in vivo* assay systems

Tatsuya Kato[1,2], Yukari Totsuka[1], Kousuke Ishino[1], Yoko Matsumoto[1,3], Yukie Tada[4], Dai Nakae[5,6], Sumio Goto[3], Shuichi Masuda[2], Sayaka Ogo[7], Masanobu Kawanishi[7], Takashi Yagi[7], Tomonari Matsuda[8], Masatoshi Watanabe[9], & Keiji Wakabayashi[2]

[1]Division of Cancer Development System, National Cancer Center Research Institute, Chuo-ku, Tokyo, Japan, [2]Graduate School of Nutritional and Environmental Sciences, University of Shizuoka, Yada, Shizuoka, Japan, [3]Laboratory of Environmental Risk Evaluation, School of Life and Environmental Science, Azabu University, Sagamihara, Kanagawa, Japan, [4]Department of Environmental Health and Toxicology, Tokyo Metropolitan Institute of Public Health, Shinjuku-ku, Tokyo, Japan, [5]Department of Pharmaceutical Sciences, Tokyo Metropolitan Institute of Public Health, Shinjuku-ku, Tokyo, Japan, [6]Tokyo University of Agriculture, Setagaya-ku, Tokyo, Japan, [7]Graduate School of Science, Osaka Prefecture University, Sakai, Osaka, Japan, [8]Research Center for Environmental Quality Management, Kyoto University, Otsu, Shiga, Japan and [9]Division of Materials Science and Engineering, Graduate School of Engineering, Yokohama National University, Hodogaya-ku, Yokohama, Japan

Abstract

The genotoxic effects of multi-walled carbon nanotubes (MWCNTs) were examined by using *in vitro* and *in vivo* assays. MWCNTs significantly induced micronuclei in A549 cells and enhanced the frequency of sister chromatid exchange (SCE) in CHO AA8 cells. When ICR mice were intratracheally instilled with a single dose (0.05 or 0.2 mg/animal) of MWCNTs, DNA damage of the lungs, analysed by comet assay, increased in a dose-dependent manner. Moreover, DNA oxidative damage, indicated by 8-oxo-7,8-dihydro-2′-deoxyguanosine and heptanone etheno-deoxyribonucleosides, occurred in the lungs of MWCNT-exposed mice. The *gpt* mutation frequencies significantly increased in the lungs of MWCNT-treated *gpt* delta transgenic mice. Transversions were predominant, and G:C to C:G was clearly increased by MWCNTs. Moreover, many regions immunohistochemically stained for inducible NO synthase and nitrotyrosine were observed in the lungs of MWCNT-exposed mice. Overall, MWCNTs were shown to be genotoxic both in *in vitro* and *in vivo* tests; the mechanisms probably involve oxidative stress and inflammatory responses.

Keywords: Micronuclei, sister chromatid exchange, DNA damage, *gpt* mutation, oxidative stress

Introduction

Multi-walled carbon nanotubes (MWCNTs) are among the most extensively researched and developed nanomaterials, finding use in electrochemical devices and for many biomedical applications. Accordingly, the market for MWCNTs is predicted to grow on a global scale and would be released into the human environment and subsequent inhalation would occur, especially in workplaces. Since MWCNTs are not only nanosized particles, but also rod-shaped fibres with a superbly high aspect ratio, their carcinogenic potential have attracted attention over the years. In fact, mesothelioma could be induced by a single intraperitoneal administration of MWCNTs in both cancer susceptible $p53^{+/-}$ mice and F344 rats (Takagi et al. 2008; Sakamoto et al. 2009). Although intraperitoneal application is not relevant to human exposure, the findings point to possible major hazard.

Due to high cost and the need for special equipment for inhalation studies to create mock conditions for the situation of human exposure, only a few reports on MWCNT inhalation are available so far (Porter et al. 2010; Morimoto et al. 2011). On the other hand, intratracheal instillation is less expensive and more easily performed, and there have been several reports of MWCNT exposure by this route using rats (Takaya et al. 2010; Reddy et al. 2012; Morimoto et al. 2011). MWCNTs induced strong inflammatory reactions, including formation of granulomas and fibrosis in the lungs. Translocation into lung-associated lymph nodes was also observed in mice and rats with both inhalation and intratracheal exposure (Porter et al. 2010, 2002; Ellinger-Ziegelbauer & Pauluhn 2009; Pauluhn 2010a). In addition to MWCNT-induced pulmonary toxicity, genotoxicity, such as micronucleus induction, chromosome aberration and DNA damage, using *in vitro* and *in vivo* assay systems have been reported and are a little controversial (Wirnitzer et al. 2009; Asakura et al. 2010; Ghosh et al. 2011; Patlolla et al. 2010a,b,c; Migliore et al. 2010). For example, Wirnitzer et al. reported

Correspondence: K. Wakabayashi, PhD, Graduate School of Nutritional and Environmental Sciences, University of Shizuoka, 52-1, Yada, Shizuoka 422-8526, Japan. Tel: +81 54 264 5784. Fax: +81 54 264 5904. E-mail: kwakabayashi@u-shizuoka-ken.ac.jp

(Received 13 December 2011; accepted 6 March 2012)

that MWCNTs demonstrated neither cytotoxic, clastogenic activities against mammalian cells nor bacteriotoxic, mutagenic activities for bacterial strains. However, most reports revealed that MWCNTs, indeed, are genotoxic and clastogenic for cultured mammalian cells, plants and mice. Among these, chromosomal damage by carbon nanotubes (both single-wall and multi-wall) has been well documented (Asakura et al. 2010; Muller et al. 2008; Sargent et al. 2009, 2011 unpublished data). However, *in vivo* genotoxicity including mutagenicity of MWCNTs has not been fully elucidated yet.

The present study, therefore, aimed to examine the genotoxicity/clastogenicity of this nanomaterial, MWCNTs, in both *in vitro* micronucleus and sister chromatid exchange (SCE) tests. Genotoxic effects were also examined by *in vivo* comet assay, DNA adduct formation and mutation assay using wild type and transgenic mice. In the present study, MWCNTs were, thereby, demonstrated to be genotoxic both in *in vitro* and *in vivo* tests, and possible mechanisms were also suggested. Finally, health concerns raised by the use of MWCNTs are also discussed.

Materials and methods

Materials

High-purity MWCNTs (MITSUI MWCNT-7, identical to those used in the Fischer 344 rats study of Sakamoto et al. 2009) were provided by Mitsui & Co., Ltd. (Ibaraki, Japan). MWCNTs were suspended in saline containing 0.05% Tween 80 (Nacalai Tesque, Kyoto, Japan) and sonicated well on ice. Width distribution of MWCNTs used in the present study indicated a Gaussian distribution with a peak at 90 nm, and more than 80% of particles belonged in a range of 70–110 nm. The length of MWCNTs distributed with a peak at 2 μm, and more than 70% of particles belonged in a range of 1–4 μm (Sakamoto et al. 2009). Detailed information, such as elemental contents of MWCNTs, can be found in a previous report (Sakamoto et al. 2009).

Standards of DNA adducts and their stable isotopes

8-Oxo-7,8-dihydro-2'-deoxyguanosine (8-oxodG) was purchased from Sigma-Aldrich Japan (Tokyo, Japan). [U-$^{15}N_5$]-8-oxodG was supplied by Dr Shibutani at SUNY Stony Brook, NY, USA. 4-Oxo-2(*E*)-nonenal-derived DNA adducts, heptanone etheno-2'-deoxycytidine (HεdC), heptanone etheno-2'-deoxyguanosine (HεdG) and heptanone etheno-2'-deoxyadenosine (HεdA) were synthesised according to previously published methods (Rindgen et al. 1999, 2000; Pollack et al. 2003).

Micronucleus test

A micronucleus test using human lung carcinoma A549 cells (RIKEN Cell Bank, Wako, Japan) was performed, as described previously (Totsuka et al. 2009). Briefly, A549 cells were seeded in plastic cell culture dishes (ϕ60 mm) 1 day before treatment. Particles were suspended in physiological saline containing 0.05% (v/v) Tween-80 with sonication (for 5–10 min at room temperature). One volume of the suspension was mixed with nine volumes of the culture medium with serum (altogether 3.3 mL/dish), and then cells were treated at indicated concentrations for 6 h. After treatment, cells were further cultured for 42 h. Then, cells were trypsinized and counted and centrifuged. Cells were resuspended in 0.075 M KCl, and incubated for 5 min. Cells were then fixed four times in methanol:glacial acetic acid (3:1) and washed with methanol containing 1% acetic acid. Finally, cells were resuspended in methanol containing 1% acetic acid. The cell solution was dropped onto slides and the nucleus was stained by mounting with 40 μg/mL acridine orange (Nacalai Tesque) solution and immediately observed by fluorescence microscopy using blue excitation. The number of cells with micronuclei was recorded based on observation of 1000 interphase cells.

SCE test

Chinese hamster ovary (CHO) AA8 cells were cultured in RPMI 1640 (Sigma-Aldrich, Japan) supplemented with 10% foetal bovine serum (JRH Biosciences, Lenexa, KS) in a 5% CO_2 atmosphere at 37°C. The cells were treated with MWCNTs for 1 h and cultured in medium containing 10% serum and 10 μg/mL 5-bromodeoxyuridine (Sigma-Aldrich, Japan) for 26 h. Colcemid (Nacalai Tesque) was added for the last 2 h at a final concentration of 60 ng/mL. Cells were trypsinized and centrifuged, resuspended in 0.075 M KCl, and incubated for 30 min. The cells were fixed four times in methanol:glacial acetic acid (3:1). The cell solution was dropped onto slides in a Metaphase Spreader HANABI (AD Science Technology, Funabashi, Japan). The slides were soaked in 50 μg/mL Hoechst #33258 (Sigma-Aldrich, St. Louis, MO, USA). The slides were covered with 0.01 M sodium phosphate buffer (pH 7.6) and cover glasses and irradiated with black light at 365 nm for 3 h. Subsequently, slides were stained with 6% Giemsa (Merck KGaA, Darmstadt, Germany) in 0.06 M sodium phosphate buffer (pH 6.4) for 15 min. SCE was scored under a microscope. The experiments were repeated until acquiring at least 50 cells that were suitable for scoring SCEs in each dose.

Animals

Male ICR mice (6 weeks old) and guanine phosphoribosyltransferase (*gpt*) delta mice (9 weeks old) were purchased from Japan SLC (Shizuoka, Japan). The *gpt* delta mice carry ~80 copies of *lambda* EG10 DNA on each chromosome 17 on a C57BL/6J background (Nohmi & Masumura 2005). The animals were provided with food (CE-2 pellet diet; CLEA Japan, Inc., Tokyo, Japan) and tap water *ad libitum* and maintained under controlled conditions: a 12 h light/dark cycle, 22 ± 2°C room temperature and 55 ± 10% relative humidity. After quarantine for 1 week, the experiments were conducted according to the "Guidelines for Animal Experiments in the National Cancer Center" of the Committee for Ethics of Animal Experimentation of the National Cancer Center.

In vivo comet assay

Each group of five male ICR mice was intratracheally instilled with nanoparticles using a polyethylene tube under anaesthesia with 4% halothane (Takeda Chemical,

present, no data are available for activation of the Nalp3 inflammasome pathway by C_{60} and kaolin. However, it is likely that both nanoparticles can activate in the same way as asbestos and silica, because oxidative stress was increased in the lungs of treated mice. Further studies of the mechanisms of genotoxicity are needed.

Acknowledgment: We thank Mr. Naoaki Uchiya and Ms Hiroko Suzuki for excellent technical assistance. This study was supported by Grants-in-Aid for Cancer Research, for the Third-Term Comprehensive 10-Year Strategy for Cancer Control, the U.S.-Japan Cooperative Medical Science Program and for Research on Risk of Chemical Substances from the Ministry of Health, Labour, and Welfare of Japan. Kousuke Ishino is presently the recipient of a Research Resident Fellowship from the Foundation for Promotion of Cancer Research.

References

1 LaDou J, Castleman B, Frank A, Gochfeld M, Greenberg M, Huff J, Joshi TK, Landrigan PJ, Lemen R, Myers J, Soffritti M, Soskolne CL, Takahashi K, Teitelbaum D, Terracini B, Watterson A. The case for a global ban on asbestos. Environ Health Perspect. 2010; 118: 897–901.

2 Nishimori H, Kondoh M, Isoda K, Tsunoda S, Tsutsumi Y, Yagi K. Histological analysis of 70-nm silica particle-induced chronic toxicity in mice. Eur J Pharm Biopharm. 2009; 72: 626–9.

3 Nabeshi H, Yoshikawa T, Matsuyama K, Nakazato Y, Arimori A, Isobe M, Tochigi S, Kondoh S, Hirai T, Akase T, Yamashita T, Yamashita K, Yoshida T, Nagano K, Abe Y, Yoshioka Y, Kamada H, Imazawa T, Itoh N, Tsunoda S, Tsutsumi Y. Size-dependent cytotoxic effects of amorphous silica nanoparticles on Langerhans cells. Pharmazie. 2010; 65:199–201.

4 Totsuka Y, Higuchi T, Imai T, Nishikawa A, Nohmi T, Kato T, Masuda S, Kinae N, Hiyoshi K, Ogo S, Kawanishi M, Yagi T, Ichinose T, Fukumori N, Watanabe M, Sugimura T, Wakabayashi K. Genotoxicity of nano/microparticles in in vitro micronuclei, in vivo comet and mutation assay systems. Part Fibre Toxicol. 2009; 6: 23.

5 Markovic Z, Trajkovic V. Biomedical potential of the reactive oxygen species generation and quenching by fullerenes (C60). Biomaterials. 2008; 29: 3561–73.

6 Cozzi R, Ricordy R, Aglitti T, Gatta V, Perticone P, De Salvia R. Ascorbic acid and beta-carotene as modulators of oxidative damage. Carcinogenesis. 1997; 18: 223–8.

7 Jacobsen NR, Pojana G, White P, Møller P, Cohn CA, Korsholm KS, Vogel U, Marcomini A, Loft S, Wallin H. Genotoxicity, cytotoxicity, and reactive oxygen species induced by single-walled carbon nanotubes and C(60) fullerenes in the FE1-Mutatrade markMouse lung epithelial cells. Environ Mol Mutagen. 2008; 49: 476–87.

8 Shi Y, Zhang JH, Jiang M, Zhu LH, Tan HQ, Lu B, Synergistic genotoxicity caused by low concentrations of titanium dioxide nanoparticles and p,p′-DDT in human hepatocytes. Environ Mol Mutagen. 2010; 51: 192–204.

9 Blair I, DNA adducts with lipid peroxidation products, J. Biol. Chem., 2008; 283: 1545–9.

10 Chou PH, Kageyama S, Matsuda S, Kanemoto K, Sasada Y, Oka M, Shinmura K, Mori H, Kawai K, Kasai H, Sugimura H, Matsuda T. Detection of lipid peroxidation-induced DNA adducts caused by 4-oxo-2(E)-nonenal and 4-oxo-2(E)-hexenal in human autopsy tissues. Chem Res Toxicol. 2010; 23:1442–8.

11 Folkmann JK, Risom L, Jacobsen NR, Wallin H, Loft S, Møller P, Oxidatively damaged DNA in rats exposed by oral gavage to C60 fullerenes and single-walled carbon nanotubes. Environ Health Perspect. 2009; 117: 703–8.

12 Tsurudome Y, Hirano T, Yamato H, Tanaka I, Sagai M, Hirano H, Nagata N, H Itoh H, Kasai H, Changes in levels of 8-hydroxyguanine in DNA, its repair and OGG1 mRNA in rat lungs after intratracheal administration of diesel exhaust particles. Carcinogenesis. 1999; 20: 1573–6.

13 Nohmi T, Masumura K. Molecular nature of intrachromosomal deletions and base substitutions induced by environmental mutagens. Environ Mol Mutagen. 2005; 45: 150–61.

14 Negishi K, Hao W. Spectrum of mutations in single-stranded DNA phage M13mp2 exposed to sunlight: predominance of G-to-C transversions. Carcinogenesis. 1992; 9: 1615–8.

15 Akasaka S, Yamamoto K. Hydrogen peroxide induces G:C to T:A and G:C to C:G transversions in the supF gene of Escherichia coli. Mol Gen Genet. 1994; 243: 500–5.

16 Valentine MR, Rodriguez H, Termini J. Mutagenesis by peroxy radicals is dominated by transversions at deoxyguanosine: evidence for the lack of involvement of 8-oxo-dG1 and/or abasic site formation. Biochemistry. 1998; 37: 7030–8.

17 Shin CY, Ponomareva ON, Connolly L, Turker MS. A mouse kidney cell line with a G:C→C:G transversion mutator phenotype. Mutat Res. 2002; 503: 69–76.

18 Kornyushyna O, Berges AM, Muller JG, Burrows CJ. In vitro nucleotide misinsertion opposite the oxidized guanosine lesions spiroiminodihydantoin and guanidinohydantoin and DNA synthesis past the lesions using Escherichia coli DNA polymerase I (Klenow fragment). Biochemistry. 2002; 41: 15304–14.

19 Cadet J, Berger M, Buchko GW, Joshi PC, Raoul S, Ravanat JL. 2,2-Diamino-4-[(3,5-di-O-acetyl-2-deoxy-.beta.-D-erythro-pentofuranosyl)amino]-5-(2H)-oxazolone: a novel and predominant radical oxidation product of 3′,5′-di-O-acetyl-2′-deoxyguanosine. J Am Chem Soc. 1994; 116: 7403–4.

20 Goyal RN, Jain N, Garg DK. Electrochemical and enzymic oxidation of guanosine and 8-hydroxyguanosine and the effects of oxidation products in mice. Bioelectrochem Bioenergetics. 1997; 43: 105–14.

21 Ye Y, Muller JG, Luo W, Mayne CL, Shallop AJ, Jones RA, Burrows CJ. Formation of 13C-, 15N-, and 18O-labeled guanidinohydantoin from guanosine oxidation with singlet oxygen. Implications for structure and mechanism. J Am Chem Soc. 2003; 125: 13926–7.

22 Burrows CJ, Muller JG, Kornyushyna O, Luo W, Duarte V, Leipold MD, David SS. Structure and potential mutagenicity of new hydantoin products from guanosine and 8-oxo-7,8-dihydroguanine oxidation by transition metals. Environ Health Perspect. 2002; 110 Suppl 5: 713–7.

23 Kino K, Sugiyama H. UVR-induced G-C to C-G transversions from oxidative DNA damage. Mutat Res. 2005; 571: 33–42.

24 Kino K, Sugiyama H. Possible cause of G-C→C-G transversion mutation by guanine oxidation product, imidazolone. Chem Biol. 2001; 8: 369–78.

25 Kino K, Ito N, Sugasawa K, Sugiyama H, Hanaoka F. Translesion synthesis by human DNA polymerase eta across oxidative products of guanine. Nucleic Acids Symp Ser. 2004; 48: 171–2.

26 Burney S, Caulfield JL, Niles JC, Wishnok JS, Tannenbaum SR. The chemistry of DNA damage from nitric oxide and peroxynitrite. Mutat Res. 1999; 424: 37–49.

27 Porter DW, Millecchia L, Robinson VA, Hubbs A, Willard P, Pack D, Ramsey D, McLaurin J, Khan A, Landsittel D, Teass A, Castranova V. Enhanced nitric oxide and reactive oxygen species production and damage after inhalation of silica. Am J Physiol Lung Cell Mol Physiol. 2002; 283: L485–93.

28 Aust A. The role of iron in asbestos induced cancer. In: Davis JMG, Jaurand M-C, editors. Cellular and molecular effects of mineral and synthetic dusts and fibers. NATO ASI Series, Vol. H85. Berlin: Springer-Verlag; 1994. p. 53–61.

29 Mossman BT, Gee BL. Pulmonary reactions and mechanisms of toxicity of inhaled fibers. In: Gardner DE, Crapo JD, McClellan RO, editors. Toxicology of the lung. 2nd ed. New York: Raven Press; 1993. p. 371–87.

30 Dostert C, Pétrilli V, Van Bruggen R, Steele C, Mossman BT, Tschopp J. Innate immune activation through Nalp3 inflammasome sensing of asbestos and silica. Science. 2008; 320: 674–7.

31 Cassel SL, Eisenbarth SC, Iyer SS, Sadler JJ, Colegio OR, Tephly LA, Carter AB, Rothman PB, Flavell RA, Sutterwala FS. The Nalp3 inflammasome is essential for the development of silicosis. Proc Natl Acad Sci U S A. 2008; 105: 9035–40.

Table I. Sister chromatid exchange (SCE) in CHO AA8 cells following a 1 h treatment with MWCNTs.

Treatment [μg/mL]	SCEs/cell*
0†	3.87 ± 1.82
0.1	6.65 ± 1.30‡
1.0	11.3 ± 2.58‡
2.0	10.1 ± 1.52‡

*Mean ± SD of at least 50 cells; †Solvent control (treatment with 0.05% (v/v) Tween 80); ‡$p < 0.01$ (*versus* solvent control) by Student's *t*-test.

Osaka, Japan). Single doses of 0.05 or 0.2 mg/animal were employed. The control mice ($n = 5$) were instilled intratracheally with 0.1 mL of the solvent alone. The mice were sacrificed 3 h after particle administration; the lungs were removed and then used immediately for comet analysis. The alkaline comet assay was performed according to previously described procedures (Totsuka et al. 2009). Fifty cells were examined per mouse. The tail moment of DNA was automatically measured using a Comet Analyzer from Youworks Co. (Ibaraki, Japan). The distance between the centre of nucleus and centre of tail was defined as tail distance, and the fluorescence intensity of damaged area was divided by that of the whole area of cell to achieve the damage ratio. The tail moment was calculated by multiplication of tail distance and damage ratio. Furthermore, percentage of DNA in the tail, another index of DNA damage, was also calculated.

DNA adduct analysis

For DNA adduct analyses, each group of five male ICR mice was intratracheally instilled with MWCNTs at a single dose of 0.2 mg/animal, and sacrificed 3, 24, 72 or 168 h after nanoparticle administration. Control samples were obtained from the lungs of mice given vehicle. Mouse lung DNA was extracted and purified using a Gentra® Puregene™ tissue kit (QIAGEN, Valencia, CA, USA). The protocol was performed according to the manufacturer's instructions except that desferroxamine (final concentration: 0.1 mM) was added to all solutions to avoid the formation of oxidative adducts during the purification step.

DNA samples in 40 μg aliquots were digested into their constituent 2'-deoxyribonucleoside-3'-monophosphate units by the addition of 15 μL of 17 mM citrate plus 8 mM $CaCl_2$ buffer that contained micrococcal nuclease (22.5 U) and spleen phosphodiesterase (0.075 U) plus internal standards. The solutions were mixed and incubated for 3 h at 37°C, then alkaline phosphatase (1 U), 10 μL of 0.5 M Tris-HCl (pH 8.5), 5 μL of 20 mM $ZnSO_4$ and 67 μL of distilled water were added and the reactions were incubated for a further 3 h at 37°C. The digested sample was extracted twice with methanol. The methanol fractions were evaporated to dryness, resuspended in 50 μL of distilled water and subjected to liquid chromatography tandem mass spectrometry (LC/MS/MS). LC/MS/MS analyses were performed using a Waters 2795 LC system (Waters, Manchester, UK) interfaced with a Quattro Ultima triple stage quadrupole MS (Waters). The LC column was eluted over a gradient that began at a ratio of 5% methanol to 95% water, changed to 30% methanol over a period of 30 min, changed to 85% methanol from 30 to 45 min, and was then maintained at 85% methanol from 45 to 55 min. Sample injection volumes of 20 μL each were separated on a Shim-pack FC-ODS column (150 × 4.6 mm, 3 μm, Shimadzu, Kyoto, Japan) and eluted at a flow rate of 0.4 mL/min. Mass spectral analyses were carried out in positive ion mode with nitrogen as the nebulising gas. The ion source temperature was 130°C; the desolvation gas temperature was 380°C. Nitrogen gas was also used as the desolvation gas (700 L/h) and cone gas (35 L/h) and argon was used to provide a collision cell pressure of 1.5×10^{-3} mbar. Positive ions were acquired in multiple reaction monitoring mode. The multiple reaction monitoring transitions were monitored; each cone voltage and collision energy used was as follows: 8-oxodG [284->168, 35 V, 14 eV], HɛdG [404->288, 35 V, 10 eV], HɛdA [388->272, 35 V, 10 eV], HɛdC [364->248, 35 V, 10 eV].

gpt and Spi⁻ mutation assays

For mutation analysis, each group of six to seven male *gpt* delta mice was intratracheally instilled with particles at a single dose or multiple doses of 0.2 mg/animal as follows. Group 1 served as the vehicle control (0.1 mL of saline containing 0.05% Tween 80), Groups 2–4 were the study groups and received single or multiple doses of MWCNTs (Group 2: single dose of 0.2 mg/animal; Group 3: 0.2 mg/animal for each of two instillations 2 weeks apart; Group 4: 0.2 mg/animal, once a week for 4 weeks). The mice were sacrificed at 22 weeks of age; this was 8–12 weeks after particle administration. Lungs were removed, and stored at −80°C until high-molecular-weight genomic DNA was extracted using a RecoverEase DNA Isolation Kit (Stratagene, La Jolla, CA, USA), according to the manufacturer's instructions. *Lambda* EG10 phages were rescued using Transpack Packaging Extract (Stratagene). The *gpt* and Spi⁻ mutagenesis assay was performed, according to previously described methods (Nohmi et al. 2000).

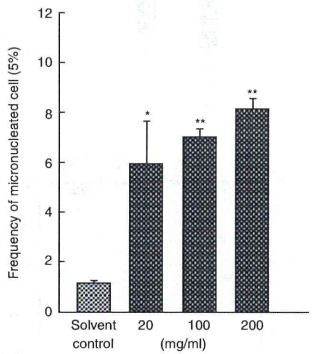

Figure 1. Frequency of micronucleated A549 cells. The frequency was calculated after counting the number of cells with micronuclei based on observation of 1000 interphase cells. Mean values ± SD of three independent experiments are shown. Solvent control represents treatment with 0.05% (v/v) Tween 80; *$p < 0.05$ and **$p < 0.01$, by Student's *t*-test.

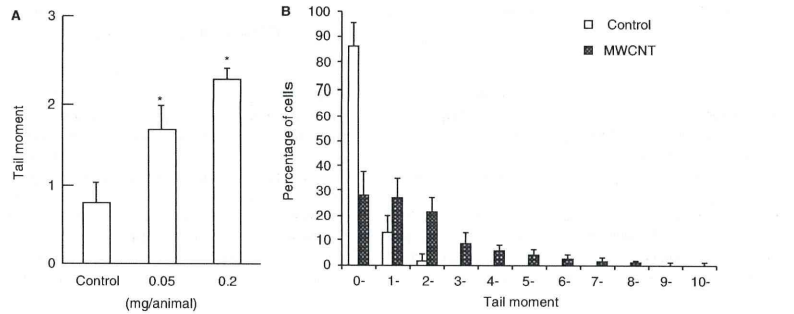

Figure 2. DNA damage in the lungs of ICR mice intratracheally instilled with MWCNTs. DNA damage was measured by comet assay. (A) The mean values of DNA tail moment in the lungs with or without a 3 h MWCNT treatment at 0.05 or 0.2 mg/animal. The values represent the mean of five animals ± SD; *$p < 0.01$, by Dunnett's test after one-way analysis of variance *versus* the corresponding vehicle control mice. (B) The percentages of cells containing a given comet tail moment at a dose of 0.2 mg/animal.

Histopathological evaluation

For histopathological evaluation, lungs obtained from *gpt* delta mice with or without nanoparticle instillation ($n = 2$ or 3) were fixed in 10% neutral buffered formalin, embedded in paraffin blocks, and routinely processed to haematoxylin and eosin-stained sections.

Immunohistochemical analysis of inflammation factors

To investigate nitric oxide production after nanoparticle exposure, immunohistochemical staining of inflammation factors, such as inducible NO synthase (iNOS) and nitrotyrosine (NT), in the lungs of *gpt* delta mice treated with MWCNTs were examined, using a procedures reported previously (Totsuka et al. 2010; Porter et al. 2002).

Statistical analysis

The data obtained from the comet assay were expressed as the mean ± standard deviation (SD). Dunnett's test after one-way analysis of variance was used to test for significant differences in tail moment and percentage of DNA in tail. The data from the micronucleus test were expressed as the mean ± SD of three independent experiments. The data from the SCE test were expressed as the mean ± SD of at least 50 cells. The data from the *gpt* and Spi⁻ mutation assays were expressed as the mean ± SD. The data were statistically compared with the corresponding solvent control using the F test before application of the Student's *t*-test. Mutational spectra were compared using Fisher's exact test (Carr & Gorelick 1996). *P* values < 0.05 were considered to indicate statistical significance.

Results

Micronucleus test

To investigate the genotoxicity/clastogenicity of MWCNTs, micronucleus-inducing activity was analysed using a human lung cancer cell line, A549. A 6 h treatment with MWCNTs, at a concentration of 20 μg/mL or higher, inhibited A549 cell growth to around 70% of control levels. As shown in Figure 1, MWCNTs increased the number of micronucleated cells in a dose-dependent manner. The frequency of micronucleated cells in the solvent control was 1.12% and the frequency rose to 8.6% in the 200 μg/mL MWCNT group. Even treatment of 20 μg/mL MWCNT induced micronuclei exceedingly, and these increases were statistically significant ($p < 0.05$).

SCE test

Table I shows the SCE frequency in CHO cells following a 1 h treatment with MWCNTs. An SCE frequency approximately three times the control level was observed in cultures treated with 1.0 μg/mL MWCNTs. This increase was statistically significant ($p < 0.01$) at 0.1 μg/mL or higher concentrations.

In vivo genotoxicity analysed by alkaline comet assay

DNA damage induced by MWCNTs in the lungs was evaluated using a comet assay under alkaline conditions. Figure 2A shows the mean values of DNA tail moment in the lungs with or without a 3 h MWCNT treatment at 0.05 or 0.2 mg/animal. DNA damage observed in the MWCNT-treated group was dose-dependent, and the values of DNA tail moment were significantly increased compared with those of the vehicle control. Also, similar dose-dependent manner was observed in the values of percentage of DNA in the tail (Supplementary Figure 1). Figure 2B shows the percentages of cells containing a given comet tail moment at a dose of 0.2 mg/animal. The numbers of damaged cells were increased by treatment with nanoparticles and damaged cells with high DNA tail moment being extremely rare in the vehicle group.

Quantification of oxidative and lipid peroxide-related DNA adducts

Levels of the DNA adduct analysed in lung DNA extracted from MWCNT-treated mice at 3, 24, 72 and 168 h after exposure are shown in Figure 3. DNA adducts related to oxidative stress and lipid peroxidation (8-oxodG, HɛdA, HɛdC, HɛdG) were all, except HɛdG, increased up to 72 h and then slightly less so at 168 h. 8-OxodG was more

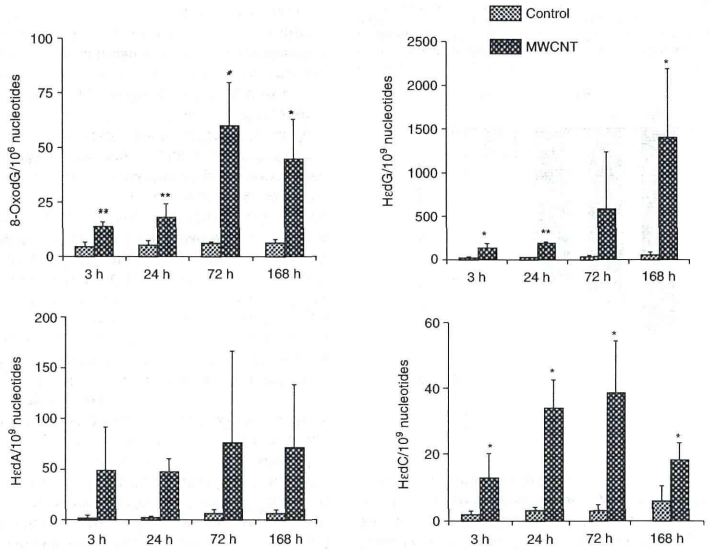

Figure 3. Oxidative and lipid peroxide-related DNA adduct formation induced by MWCNT exposure in the lungs of ICR mice. DNA was extracted from the lungs 3, 24, 72 and 168 h after intratracheal instillation of 0.2 mg of MWCNTs, and was enzymatically digested. Control samples were obtained from the lungs of mice given vehicle for the same durations of MWCNT exposure. 8-OxodG and three types of Hε-adduct were quantified by stable isotope dilution LC-MS/MS. Asterisks (*, **) indicate a significant difference ($p < 0.05$, < 0.01) from vehicle control (treatment with 0.05% (v/v) Tween-80) at same point in the Student's *t*-test.

abundantly found than the Hε–adduct derived from lipid peroxidation.

General observations and histopathological evaluation of *gpt* delta transgenic mice administered with MWCNTs

The body weights of *gpt* delta mice in the vehicle control group were 34.9 ± 1.9 g at the end of the experiment. The body weights of the *gpt* delta mice that received single or multiple doses of 0.2 mg MWCNTs were 75–80% of those in the vehicle control group during or just after the instillations, then gradually returned to normal by the end of the experiment.

There were no obvious histopathological changes in the lungs of Group 1 control mice (Figure 4A). In mice given a single MWCNT administration (0.2 mg/animal; Group 2), infiltration of macrophages phagocytising tubes in the alveolar lumina and walls, and granulation with fibrosis were observed, in association with inflammatory lymphocyte infiltration in macrophage-clustered lesions and around the vessels and bronchi (Figure 4B). Degeneration, enhanced secretion and hyperplasia were found in the bronchial epithelia, and type II alveolar epithelial cells appeared hyperplastic (Figure 4B). The thickening lesions were also seen in the visceral pleurae, which were due to sub-pleural fibrosis with the occasional detection of MWCNTs (Figure 4D and 4E). When MWCNTs were multiply administered (0.2 mg weekly for 4 weeks; Group 4), generally similar findings were observed but with a much higher severity (Figure 4C). Moreover, MWCNTs were deposited in the paratracheal lymph nodes (Figure 4F). Similar findings, but with a slighter degree of particle accumulation and granuloma formation, were observed in the lungs of mice that received two consecutive MWCNT instillations (Group 3; data not shown).

gpt and Spi$^-$ mutations in the lungs of *gpt* transgenic mice treated with MWCNTs

The *gpt* delta transgenic mice were exposed to single or multiple intratracheal instillations of 0.2 mg MWCNTs and the mutations in the lungs were analysed. Data are summarised in Supplementary Table I, and Figure 5 shows the *gpt* mutant frequencies (MFs) in the lungs. The background MF of the lungs was $7.53 \pm 0.91 \times 10^{-6}$. There was no increase in the MF in lungs exposed to single or double doses of MWCNTs. However, four instillations of MWCNTs resulted in a significant increase in the MF, of approximately two-fold compared with that in controls (Figure 5). The Spi$^-$ MFs were measured in the lungs of *gpt* delta mice instilled with MWCNTs, but no increases were observed (data not shown).

To analyse the characteristics of the mutations induced by MWCNTs, the authors tested for 6-thioguanine (6-TG)-resistant mutants using PCR and DNA sequencing analysis. A total of 42 independent 6-TG-resistant mutants derived

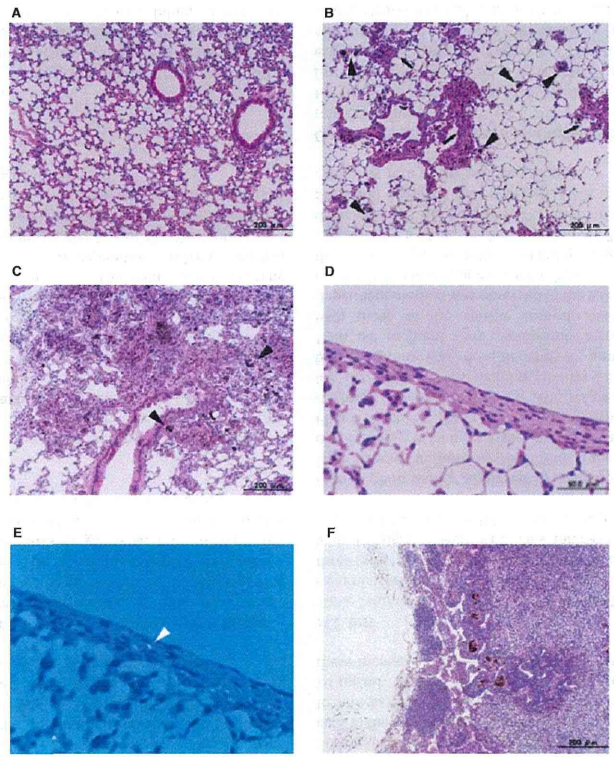

Figure 4. Representative histopathology of the lungs of (A) a control mouse given vehicle (once a week for 4 weeks; killed at the end of month 3); (B) a mouse given a single dose of 0.2 mg MWCNTs (killed at the end of month 3); (C) a mouse given multiple doses of 0.2 mg MWCNTs (once a week for 4 weeks; killed at the end of month 3); (D) a mouse given MWCNT (0.2 mg/head, singly, killed at the end of month 3); (E), a polarisation photomicrograph serial to (D); and (F) a representative paratracheal lymph node of a mouse given multiple doses of 0.2 mg MWCNTs (once a week for 4 weeks; killed at the end of month 3). MWCNT-phagocytised macrophages (black arrowheads) can be observed, and granulation with fibrosis (black arrows) is also found in lungs of MWCNT-instilled mice. In polarisation photomicrograph, MWCNTs is indicated by white arrowhead.

from MWCNT instillations were identified and 24 mutants were identified from vehicle controls. The classes of mutation found in the *gpt* gene are summarised in Table II. Base substitutions predominated in nanoparticle-induced and spontaneous cases. No G:C to C:G transversions were detected in the vehicle control group; however, this type of mutation could be detected in several MWCNT-instilled animals, and p value can be considered significant ($p < 0.05$). The numbers of A:T to T:A transversions and deletions were also slightly increased by MWCNT treatment, though p values were not significant.

Immunohistochemical analysis of inflammation factors

As shown in Figure 6, the pattern of iNOS and NT staining corresponded to the areas of inflammation within the lung parenchyma. In the case of MWCNT exposure, many regions of the lungs stained positively, and intense iNOS and NT staining was mainly localised in test substance-phagocytised macrophages and granulomas (indicated by green arrows). Some alveolar epithelial cells located near granulomas were also stained positive for the iNOS and NT antibodies (indicated by arrowheads). In contrast, no regions stained positively for iNOS were observed in the lungs of vehicle control mice (Figure 6D). Similar results were obtained for vehicle control mice immunoreaction with NT (data not shown).

Discussion

The present study showed MWCNTs to clearly exert genotoxicity in *in vitro* assay systems, significantly inducing

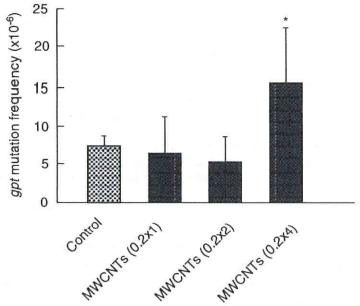

Figure 5. The *gpt* MFs in the lungs of mice after single and multiple intratracheally instillations of MWCNTs. Male mice were treated with a single (0.2 mg) or multiple (0.2 mg × 2 or 4) doses of particles, and mice were sacrificed 12 (single-dose) or 8 (multiple-dose) weeks after particle administration. The data represent the mean ± SD; $^{*}p < 0.05$ by Student's *t*-test *versus* the corresponding vehicle control mice.

micronuclei and enhancing the frequency of SCEs in A549 and CHO AA8 cells. Consistent with this, several studies have reported that MWCNTs can be taken up into many types of cells and demonstrate genotoxicity, including human epithelial lung cells (Wörle-Knirsch et al. 2006), mesothelioma cells (Wick et al. 2007), keratinocytes (Monteiro-Riviere et al. 2005), and normal dermal fibroblast cells (Patlolla et al. 2010b). Recently, several reports have demonstrated that carbon nanotubes induce both clastogenic events and aneugenic events (Muller et al. 2008; Sargent et al. 2009, 2011 unpublished data). Indeed, one of the mechanisms of genotoxicity is considered to be the disruption of mitotic spindles by association with mitotic tubules (Sargent et al. 2009, 2011 unpublished data; Asakura et al. 2010). Moreover, a direct interaction between carbon nanotubes and DNA has also been reported (Li et al. 2005). Other than that, it has been reported that modified gold nanoparticles induce the unfolding of fibrinogen *via* binding and then promote interaction with the integrin receptor Mac1 and induce the release of inflammatory cytokines (Deng et al. 2011). In the present study, no data are available to explain the exact mechanisms of *in vitro* genotoxicity by MWCNTs; however, direct interaction between biomolecules, such as protein and DNA, and MWCNTs might be partly involved for induction of the *in vitro* genotoxicity.

In addition to the *in vitro* genotoxicity, MWCNTs were showed to be genotoxic in the lungs of mice using a comet assay. Under similar conditions, levels of 8-oxodG were significantly increased in MWCNT-treated mice, and the level was maintained for 1 week. The levels of HεdA, HεdC and HεdG also tended to increase. These DNA adducts are derived from lipid peroxidation, suggesting that MWCNTs may induce oxygenation of lipids in tissues caused by generation of reactive oxygen species (ROS). Consistently, it has been reported that the levels of lipid hydroperoxides, which are prominent non-radical intermediates of lipid peroxidation products, were increased in the liver of Swiss-Webster mice intraperitoneally administered with MWCNTs (Patlolla et al. 2010c). Moreover, in the present study, MWCNTs showed mutagenicity in the lungs of *gpt* delta transgenic mice. However, a dose-dependent MF increase was not observed in the lungs of MWCNT-treated groups. The reason is still unclear, but weak responses observed in single or double doses suggested that the degree of DNA damage seems insufficient to fix as mutations, therefore it could not raise MFs more than basal levels under these conditions. Supporting this hypothesis, previous reports have revealed that obvious responses were not observed in either cellular inflammatory end points in bronchoalveolar lavage or pathological changes, such as immune response and fibrosis, in the lungs of animals exposed to low doses of MWCNTs (Ryman-Rasmussen et al. 2009; Pauluhn 2010a). On the other hand, it has also been reported that MWCNTs are difficult to eliminate; it remain in the lungs for a long time and trigger sustained pulmonary inflammation (Ellinger-Ziegelbauer & Pauluhn 2009; Pauluhn 2010a,b). Therefore, to evaluate the effects of MWCNTs with low exposure, it would be preferable to use long-term mutation assay systems. In general, 8-oxodG causes transversion

Table II. Classification of *gpt* mutations isolated from the lungs of control and MWCNT-treated mice.

	Control		MWCNTs		
Type of mutation	No. of mutants (%)	Specific MF† (× 10^{-6})	No. of mutants (%)	Specific MF† (× 10^{-6})	*p* value*
Base substitution					
Transition					
G:C to A:T	7 (29.2)	2.20	11 (26.2)	4.03	0.238
A:T to G:C	2 (8.3)	0.62	2 (4.8)	0.74	1.000
Transversion					
G:C to T:A	8 (33.3)	2.51	10 (23.8)	3.66	0.481
G:C to C:G	0 (0)	0.00	5 (11.9)	1.83	0.02
A:T to T:A	0 (0)	0.00	1 (2.4)	0.37	0.458
A:T to C:G	2 (8.3)	0.62	2 (4.8)	0.74	1.000
Insertion	1 (4.2)	0.32	2 (4.8)	0.74	0.596
Deletion	4 (16.7)	1.26	9 (21.4)	3.29	0.101
Others	0 (0)	0.00	0 (0)	0.00	-
Total	24 (100)	7.53	42 (100)	15.40	0.004

*p values were determined using Fisher's exact test according to Carr and Gorelick; †Specific MF was calculated by multiplying the total mutation frequency by the ratio of each type of mutation to the total mutation.

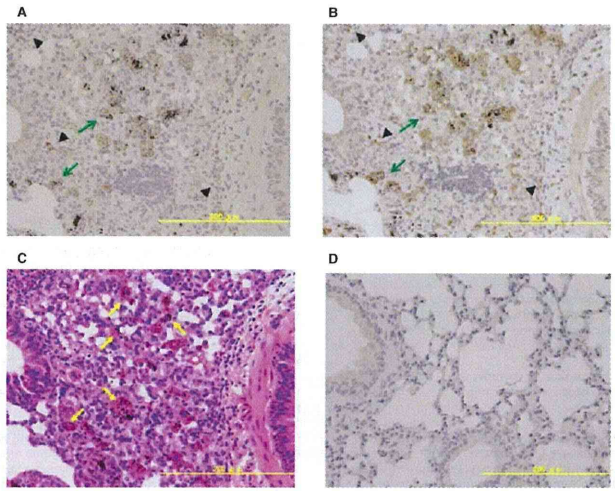

Figure 6. Immunohistochemical localisation of iNOS and NT. The panels show the alveolar region in a mouse exposed to MWCNTs, with positive staining for iNOS (A) and NT (B), and a haematoxylin and eosin stain (C). The black-coloured material is MWCNTs. Note the intense staining for iNOS and NT in both the granulomatous regions (green arrows) and epithelial cells (black arrowheads). The granulomatous regions in (C) are indicated by yellow arrows. Panel (D) shows the alveolar region in a vehicle control mouse with no significant staining for iNOS. Scale bars = 200 μm.

mutations (G:C to T:A) in DNA because it can base pair with adenine as well as cytosine (Shibutani et al. 1991; Moriya 1993). Recently, it has been reported that HεdC predominantly induces C to A or T mutations in human cells (Pollack et al. 2006; Yang et al. 2009). However, the most prominent mutation type induced by MWCNTs was G:C to C:G transversions, as was the case in our previous reports on fullerene and kaolin (Totsuka et al. 2009). In addition, Jacobsen et al. have recently reported that carbon black (Printex 90) induced base substitutions in the *cII* gene in FE1-Muta™Mouse lung epithelial cells (Jacobsen et al. 2011). The significant increases in these mutations were G:C to T:A, G:C to C:G and A:T to T:A, being similar to the results. Moreover, these mutations might be considered a hallmark of oxidative stress conditions. Oxidative products of guanine other than 8-oxodG, such as imidazolone, oxazolone (Oz), spiroiminodihydantoin, (Sp) and guanidinohydantoin (Gh), are now thought to be important causes of G to C transversions in translesion synthesis systems (Kornyushyna et al. 2002; Cadet et al. 1994; Goyal et al. 1997; Ye et al. 2003; Burrows et al. 2002; Kino & Sugiyama 2005, 2001; Kino et al. 2004). Therefore, it is suggested that Oz, Sp and Gh formation by MWCNTs might contribute to induce G:C to C:G transversions. Thus, it is important to analyse the formation of Oz, Sp and Gh in the lungs of mice treated with MWCNTs. The following hypotheses can be suggested to account for the *in vivo* genotoxic effects of MWCNTs through oxidative stress: (i) nanoparticles might trigger ROS production by iron-catalysed Fenton reactions; or (ii) nanoparticles could accumulate in cells because of phagocytosis and then enhance the production of ROS by NADPH oxidase (Aust 1994; Mossman & Gee 1993).

In the present study, inflammatory changes were introduced in the lungs of MWCNT-treated mice. Histologically, the infiltration of macrophages phagocytising tubes is thought to be a trigger, and it is clear that this inflammation originates from the host reaction towards foreign bodies. Bronchial and alveolar epithelia were influenced secondarily. It is noteworthy that the induction of lung inflammation was dependent on the total administered dose of MWCNTs. These histological findings are in line with those in previous reports indicating the induction of inflammation in the lungs by MWCNTs (Aiso et al. 2010; Ma-Hock et al. 2009; Pacurari et al. 2010; Poland et al. 2008; Takagi et al. 2008; Sakamoto et al. 2010). Intratracheally administered MWCNTs were shown to reach the visceral pleura, causing its thickening (Ryman-Rasmussen et al. 2009). Moreover, nitric oxide is known to be produced by activated macrophages in inflamed organs (Porter et al. 2006). In fact, iNOS- and NT-positive regions were frequently observed in the lungs of mice exposed to MWCNTs not only in test substance-phagocytised macrophages and granulomas but also in alveolar cells located near substance-phagocytised macrophages and granulomas (Figure 6, indicated by arrowheads). This suggests that MWCNTs induce nitric oxide production and gene mutation in the surrounding alveolar epithelial cells. Moreover, MWCNTs were found in the regional lymph nodes; such tubes would enter the lymphatic circulation and may then be distributed systemically.

Recently, many types of modified MWCNTs have been produced because of increases in their functionality and

more widespread use (Chen et al. 2010). However, the genotoxicity of these modified nanomaterials has yet to be examined. Recent data have shown that the acute toxicity and genotoxicity of MWCNTs could be eliminated by the induction of structural defects after high-temperature treatment (Fenoglio et al. 2008). It has also been reported that MWCNT-induced toxicity, such as oxidative stress and inflammation, was increased by acid-based polymer coating but that coating MWCNTs with a polystyrene-based polymer protected against toxicity (Tabet et al. 2011). To improve their safety for occupational and general users, it is necessary to clarify the genotoxicity of modified MWCNTs.

Conclusions

It has been clearly demonstrated that MWCNTs induce both *in vitro* and *in vivo* genotoxicity. Although the mechanisms are not yet fully understood, oxidative stress and inflammation are likely to be involved. Thus, further studies of the mechanisms of genotoxicity are needed. Moreover, the levels of human exposure to MWCNTs should be studied to enable evaluation of the risk of MWCNTs to human health.

Acknowledgments

We thank Mr Naoaki Uchiya and Ms Hiroko Suzuki for excellent technical assistance.

Declaration of interest

The authors report no conflicts of interest. The authors alone are responsible for the content and writing of the paper. This study was supported by Grants-in-Aid for Cancer Research, for the U.S. – Japan Cooperative Medical Science Program, for Research on Risk of Chemical Substances from the Ministry of Health, Labour, and Welfare of Japan, for Young Scientists (B) 23710084, KAKENHI (23221006) and for the Global COE Program from the Ministry of Education, Culture, Sports, Science and Technology of Japan. The study was also supported by a grant from the Japan Chemical Industry Association (JCIA) Long-range Research Initiative (LRI). Kousuke Ishino is presently the recipient of a Research Resident Fellowship from the Foundation for Promotion of Cancer Research. The findings and conclusions in this manuscript have not been formally disseminated by the University of Shizuoka and should not be construed to represent any agency determination or policy.

References

Aiso S, Yamazaki K, Umeda Y, Asakura M, Kasai T, Takaya M, Toya T, et al. 2010. Pulmonary toxicity of intratracheally instilled multiwall carbon nanotubes in male Fischer 344 rats. Ind Health 48:783–795.

Asakura M, Sasaki T, Sugiyama T, Takaya M, Koda S, Nagano K, et al. 2010. Genotoxicity and cytotoxicity of multi-wall carbon nanotubes in cultured Chinese hamster lung cells in comparison with chrysotile A fibers. J Occup Health 52:155–166.

Aust A. 1994. The role of iron in asbestos induced cancer. In: Davis JMG, Jaurand M-C, editors. Cellular and Molecular Effects of Mineral and Syntheticn Dusts and Fibers. NATO ASI Series. Vol. H85. Berlin: Springer-Verlag. pp 53–61.

Burrows CJ, Muller JG, Kornyushyna O, Luo W, Duarte V, Leipold MD, et al. 2002. Structure and potential mutagenicity of new hydantoin products from guanosine and 8-oxo-7,8-dihydroguanine oxidation by transition metals. Environ Health Perspect 110 (Suppl 5):713–717.

Cadet J, Berger M, Buchko GW, Joshi PC, Raoul S, Ravanat JL. 1994. 2,2-Diamino-4-[(3,5-di-O-acetyl-2-deoxy-.beta.-D-erythro- pentofuranosyl)amino]-5-(2H)-oxazolone: a novel and predominant radical oxidation product of 3',5'-di-O-acetyl-2'-deoxyguanosine. J Am Chem Soc 116:7403–7404.

Carr GJ, Gorelick NJ. 1996. Mutational spectra in transgenic animal research: data analysis and study design based upon the mutant or mutation frequency. Environ Mol Mutagen 28:405–413.

Chen CH, Su HC, Chuang SC, Yen SJ, Chen YC, Lee YT, et al. 2010. Hydrophilic modification of neural microelectrode arrays based on multi-walled carbon nanotubes. Nanotechnology 21:485501.

Deng ZJ, Liang M, Monteiro M, Toth I, Minchin RF. 2011. Nanoparticle-induced unfolding of fibrinogen promotes Mac-1 receptor activation and inflammation. Nat Nanotechnol 6:39–44.

Ellinger-Ziegelbauer H, Pauluhn J. 2009. Pulmonary toxicity of multi-walled carbon nanotubes (Baytubes) relative to alpha-quartz following a single 6h inhalation exposure of rats and a 3 months post-exposure period. Toxicology 266:16–29.

Fenoglio I, Greco G, Tomatis M, Muller J, Raymundo-Piñero E, Béguin F, et al. 2008. Structural defects play a major role in the acute lung toxicity of multiwall carbon nanotubes: physicochemical aspects. Chem Res Toxicol 21:1690–1697.

Ghosh M, Chakraborty A, Bandyopadhyay M, Mukherjee A. 2011. Multi-walled carbon nanotubes (MWCNT): induction of DNA damage in plant and mammalian cells. J Hazard Mater. 197:327–36.

Goyal RN, Jain N, Garg DK. 1997. Electrochemical and enzymic oxidation of guanosine and 8-hydroxyguanosine and the effects of oxidation products in mice. Bioelectrochemistry Bioenerg 43:105–114.

Jacobsen NR, White PA, Gingerich J, Møller P, Saber AT, Douglas GR, et al. 2011. Mutation spectrum in FE1-MUTA(TM) Mouse lung epithelial cells exposed to nanoparticulate carbon black. Environ Mol Mutagen 52:331–337.

Kino K, Ito N, Sugasawa K, Sugiyama H, Hanaoka F. 2004. Translesion synthesis by human DNA polymerase eta across oxidative products of guanine. Nucleic Acids Symp Ser 48:171–172.

Kino K, Sugiyama H. 2001. Possible cause of G-C->C-G transversion mutation by guanine oxidation product, imidazolone. Chem Biol 8:369–378.

Kino K, Sugiyama H. 2005. UVR-induced G-C to C-G transversions from oxidative DNA damage. Mutat Res 571:33–42.

Kornyushyna O, Berges AM, Muller JG, Burrows CJ. 2002. In vitro nucleotide misinsertion opposite the oxidized guanosine lesions spiroiminodihydantoin and guanidinohydantoin and DNA synthesis past the lesions using Escherichia coli DNA polymerase I (Klenow fragment). Biochemistry 41:15304–15314.

Li S, He P, Dong J, Guo Z, Dai L. 2005. DNA-directed self-assembling of carbon nanotubes. J Am Chem Soc. 127:14–5.

Ma-Hock L, Treumann S, Strauss V, Brill S, Luizi F, Mertler M, et al. 2009. Inhalation toxicity of multiwall carbon nanotubes in rats exposed for 3 months. Toxicol Sci 112:468–481.

Migliore L, Saracino D, Bonelli A, Colognato R, D'Errico MR, Magrini A, et al. 2010. Carbon nanotubes induce oxidative DNA damage in RAW 264.7 cells. Environ Mol Mutagen 51 (4):294–303.

Monteiro-Riviere NA, Inman AO, Wang YY, Nemanich RJ. 2005. Surfactant effects on carbon nanotube interactions with human keratinocytes. Nanomedicine 1:293–299.

Morimoto Y, Hirohashi M, Ogami A, Oyabu T, Myojo T, Todoroki M, et al. 2011. Pulmonary toxicity of well-dispersed multi-wall carbon nanotubes following inhalation and intratracheal instillation. Nanotoxicology; doi: 10.3109/17435390.2011.594912, 29 June 2011.

Moriya M. 1993. Single-stranded shuttle phagemid for mutagenesis studies in mammalian cells: 8-oxoguanine in DNA induces targeted G.C->T.A transversions in simian kidney cells. Proc Natl Acad Sci USA 90:1122–1126.

Mossman BT, Gee BL. 1993. Pulmonary reactions and mechanisms of toxicity of inhaled fibers. In: Gardner DE, et al. editors. Toxicology of the Lung. 2nd ed. New York: Raven Press. pp 371–387.

Muller J, Decordier I, Hoet PH, Lombaert N, Thomassen L, Huaux F, et al. 2008. Clastogenic and aneugenic effects of multi-wall carbon nanotubes in epithelial cells. Carcinogenesis 29:427–433.

Nohmi T, Masumura K. 2005. Molecular nature of intrachromosomal deletions and base substitutions induced by environmental mutagens. Environ Mol Mutagen 45:150–161.

Nohmi T, Suzuki T, Masumura K. 2000. Recent advances in the protocols of transgenic mouse mutation assays. Mutat Res 455:191–215.

Pacurari M, Castranova V, Vallyathan V. 2010. Single- and multi-wall carbon nanotubes versus asbestos: are the carbon nanotubes a new health risk to humans? J Toxicol Environ Health A 73:378–395.

Patlolla A, Hussain SM, Schlager JJ, Patlolla S, Tchounwou PB. 2010c. Comparative study of the clastogenicity of functionalized and nonfunctionalized multiwalled carbon nanotubes in bone marrow cells of Swiss-Webster mice. Environ Toxicol 25:608–621.

Patlolla A, Knighten B, Tchounwou P. 2010a. Multi-walled carbon nanotubes induce cytotoxicity, genotoxicity and apoptosis in normal human dermal fibroblast cells. Ethn 20(Suppl 1):S1-65–S1-72.

Patlolla A, Patlolla B, Tchounwou P. 2010b. Evaluation of cell viability, DNA damage, and cell death in normal human dermal fibroblast cells induced by functionalized multiwalled carbon nanotube. Mol Cell Biochem 338:225–232.

Pauluhn J. 2010a. Subchronic 13-week inhalation exposure of rats to multiwalled carbon nanotubes: toxic effects are determined by density of agglomerate structures, not fibrillar structures. Toxicol Sci 113:226–242.

Pauluhn J. 2010b. Multi-walled carbon nanotubes (Baytubes): approach for derivation of occupational exposure limit. Regul Toxicol Pharmacol 57:78–89.

Poland CA, Duffin R, Kinloch I, Maynard A, Wallace WA, Seaton A, et al. 2008. Carbon nanotubes introduced into the abdominal cavity of mice show asbestos-like pathogenicity in a pilot study. Nat Nanotechnol 3:423–428.

Pollack M, Oe T, Lee SH, Silva Elipe MV, Arison BH, Blair IA. 2003. Characterization of 2'-deoxycytidine adducts derived from 4-oxo-2-nonenal, a novel lipid peroxidation product. Chem Res Toxicol 16:893–900.

Pollack M, Yang IY, Kim HY, Blair IA, Moriya M. 2006. Translesion DNA Synthesis across the heptanone-etheno-2'-deoxycytidine adduct in cells. Chem Res Toxicol 19:1074–1079.

Porter DW, Hubbs AF, Mercer RR, Wu N, Wolfarth MG, Sriram K, et al. 2010. Mouse pulmonary dose- and time course-responses induced by exposure to multi-walled carbon nanotubes. Toxicology 269:136–147.

Porter DW, Millecchia LL, Robinson VA, Hubbs A, Willard P, Pack D, et al. 2002. Enhanced nitric oxide and reactive oxygen species production and damage after inhalation of silica. Am J Physiol Lung Cell Mol Physiol 283:L485–L493.

Porter DW, Millecchia LL, Willard P, Robinson VA, Ramsey D, McLaurin J, et al. 2006. Nitric oxide and reactive oxygen species production causes progressive damage in rats after cessation of silica inhalation. Toxicol Sci 90(1):188–197.

Reddy AR, Reddy YN, Krishna DR, Himabindu V. 2012. Pulmonary toxicity assessment of multiwalled carbon nanotubes in rats following intratracheal instillation. Environ Toxicol 27:211–219.

Rindgen D, Lee SH, Nakajima M, Blair IA. 2000. Formation of a substituted 1,N(6)-etheno-2'-deoxyadenosine adduct by lipid hydroperoxide-mediated generation of 4-oxo-2-nonenal. Chem Res Toxicol 13:846–852.

Rindgen D, Nakajima M, Wehrli S, Xu K, Blair IA. 1999. Covalent modifications to 2'-deoxyguanosine by 4-oxo-2-nonenal, a novel product of lipid peroxidation. Chem Res Toxicol 12:1195–1204.

Ryman-Rasmussen JP, Cesta MF, Brody AR, Shipley-Phillips JK, Everitt JI, Tewksbury EW, et al. 2009. Inhaled carbon nanotubes reach the subpleural tissue in mice. Nat Nanotechnol 4:747–751.

Sakamoto Y, Nakae D, Fukumori N, Tayama K, Maekawa A, Imai K, et al. 2009. Induction of mesothelioma by a single intrascrotal administration of multi-wall carbon nanotube in intact male Fischer 344 rats. J Toxicol Sci 34:65–76.

Sakamoto Y, Nakae D, Hagiwara Y, Satoh K, Ohashi N, Fukamachi K, et al. 2010. Serum level of expressed in renal carcinoma (ERC)/mesothelin in rats with mesothelial proliferative lesions induced by multi-wall carbon nanotube (MWCNT). J Toxicol Sci 35:265–270.

Sargent LM, Shvedova AA, Hubbs AF, Salisbury JL, Benkovic SA, Kashon ML, et al. 2009. Induction of aneuploidy by single-walled carbon nanotubes. Environ Mol Mutagen 50:708–717.

Shibutani S, Takeshita M, Grollman AP. 1991. Insertion of specific bases during DNA synthesis past the oxidation-damaged base8-oxodG. Nature 349:431–434.

Tabet L, Bussy C, Setyan A, Simon-Deckers A, Rossi MJ, Boczkowski J, et al. 2011. Coating carbon nanotubes with a polystyrene-based polymer protects against pulmonary toxicity. Part Fibre Toxicol 8:3.

Takagi A, Hirose A, Nishimura T, Fukumori N, Ogata A, Ohashi N, et al. 2008. Induction of mesothelioma in p53+/- mouse by intraperitoneal application of multi-wall carbon nanotube. J Toxicol Sci 33:105–116.

Takaya M, Serita F, Yamazaki K, Aiso S, Kubota H, Asakura M, et al. 2010. Characteristics of multiwall carbon nanotubes for an intratracheal instillation study with rats. Ind Health 48:452–459.

Totsuka Y, Higuchi T, Imai T, Nishikawa A, Nohmi T, Kato T, et al. 2009. Genotoxicity of nano/microparticles in in vitro micronuclei, in vivo comet and mutation assay systems. Part Fibre Toxicol 6:23.

Totsuka Y, Kato T, Masuda S, Ishino K, Matsumoto Y, Goto S, et al. 2010. In vitro and in vivo genotoxicity induced by fullerene (C60) and kaolin. Genes Environ 33:14–20.

Wick P, Manser P, Limbach LK, Dettlaff-Weglikowska U, Krumeich F, Roth S, et al. 2007. The degree and kind of agglomeration affect carbon nanotube cytotoxicity. Toxicol Lett 168:121–131.

Wirnitzer U, Herbold B, Voetz M, Ragot J. 2009. Studies on the in vitro genotoxicity of baytubes, agglomerates of engineered multi-walled carbon-nanotubes (MWCNT). Toxicol Lett 186:160–165.

Wörle-Knirsch JM, Pulskamp K, Krug HF. 2006. Oops they did it again! Carbon nanotubes hoax scientists in viability assays. Nano Lett 6:1261–1268.

Yang IY, Hashimoto K, de Wind N, Blair IA, Moriya M. 2009. Two distinct translesion synthesis pathways across a lipid peroxidation-derived DNA adduct in mammalian cells. J Biol Chem 284:191–198.

Ye Y, Muller JG, Luo W, Mayne CL, Shallop AJ, Jones RA, et al. 2003. Formation of 13C-, 15N-, and 18O-labeled guanidinohydantoin from guanosine oxidation with singlet oxygen. Implications for structure and mechanism. J Am Chem Soc 125:13926–13927.

Nanotoxicology Downloaded from informahealthcare.com by National Cancer Center Library on 02/27/14
For personal use only.

Supplementary material available online

Supplementary Table I, Figure 1.

RIGHTSLINK

The Journal of Toxicological Sciences (J. Toxicol. Sci.)
Vol.38, No.3, 503-511, 2013

Original Article

Genotoxicity and reactive oxygen species production induced by magnetite nanoparticles in mammalian cells

Masanobu Kawanishi[1], Sayaka Ogo[1], Miho Ikemoto[1], Yukari Totsuka[2], Kousuke Ishino[2], Keiji Wakabayashi[3] and Takashi Yagi[1,4]

[1]Graduate School of Science and Radiation Research Center, Osaka Prefecture University, 1-2 Gakuen-cho, Sakai, Osaka 599-8570, Japan
[2]Division of Cancer Development System, National Cancer Center Research Institute, 5-1-1 Tsukiji, Chuo-ku, Tokyo, 104-0045, Japan
[3]Graduate School of Nutritional and Environmental Sciences, University of Shizuoka, 52-1 Yada, Suruga-ku, Shizuoka, 422-8002, Japan
[4]Department of Life Science, Dongguk University Seoul, 26, 3 Pil-dong, Jung-gu, Seoul, 100-715, Korea

(Received February 21, 2013; Accepted March 7, 2013)

ABSTRACT — We examined the genotoxicity of magnetite nanoparticles (primary particle size: 10 nm) on human A549 and Chinese hamster ovary (CHO) AA8 cells. Six hours' treatment with the particles dose-dependently increased the frequency of micronuclei (MN) in the A549 and CHO AA8 cells up to 5.2% and 5.0% at a dose of 200 μg/ml (34 μg/cm²), respectively. In A549 cells, treatment with the nanoparticles (2 μg/ml) for 1 hr induced H2AX phosphorylation, which is suggestive of DNA double strand breaks (DSB). Treating CHO AA8 cells with 2 μg/ml (0.34 μg/cm²) magnetite for 1 hour resulted in a five times higher frequency of sister chromatid exchange (SCE) than the control level. We detected reactive oxygen species (ROS) in CHO cells treated with the particles. These findings indicate that magnetite nanoparticles induce ROS in mammalian cells, leading to the direct or indirect induction of DSB, followed by clastogenic events including MN and SCE.

Key words: Magnetite nanoparticles, Genotoxicity, DNA damage, Reactive oxygen species, Mammalian cells

INTRODUCTION

Nanosized particles are important materials in many areas including the industrial, medical, and cosmetic fields since they have useful physical and chemical properties, such as increased chemical and/or biological reactivity, a larger active surface area, or enhanced electrical conductivity, etc. (Mazzola, 2003; Paull *et al.*, 2003; Elmore, 2003; IARC, 1996; Hoet *et al.*, 2006; Bosi *et al.*, 2003; Oberdorster *et al.*, 2005). However, these particles can be released into the environment and then inhaled by humans. Thus, occupational exposure to airborne nanoparticles has become a focus of attention in recent years. For example, their adverse effects on health have begun to be reported (Peters *et al.*, 1997; Schulz *et al.*, 2005). One of the major mechanisms by which nanosized particles cause adverse health effects is their ability to generate reactive oxygen species (ROS), which leads to oxidative stress in cells (Upadhyay *et al.*, 2003; Donaldson *et al.*, 2005). However, toxicological information on the effects of nanoparticles is still scarce (Lewinski *et al.*, 2008).

Magnetite, a mineral, is one of two common naturally occurring oxides of iron (general formula: Fe_3O_4). Nanosized magnetite particles have received special interest in the biological and medical science fields due to their superior biocompatibility, chemical stability in physiological media, and ease of production (Figuerola *et al.*, 2010). Cytotoxicity of the particles in different cell lines has been reported but to a varying extent (Ankamwar *et al.*, 2010; Hussain *et al.*, 2005; Pickard and Chari, 2010). Instillation of the particles in mice increased expression of pro-inflammatory cytokines and reduced intracellular glutathione (Park *et al.*, 2010). Several studies have examined the genotoxicity of nanosized magnetite particles; however, the data about this subject are incomplete and do

Correspondence: Takashi Yagi (E-mail: yagi-t@riast.osakafu-u.ac.jp)

not give a coherent picture. Konczol *et al.* (2011) reported that treatment with magnetite nanoparticles induced ROS production, DNA damage as measured with the comet assay, and micronuclei (MN) formation in human alveolar epithelial-like type-II cells (A549 cells). On the other hand, they did not cause a significant increase in DNA damage or MN formation in Syrian hamster embryo cells (Guichard *et al.*, 2012). Size of the particles used by both groups was almost the same; Konczol *et al.* used the particles with 20-60 nm and Guichard *et al.* used those with 27 ± 8 nm. Their chemical purities were similar as well (≥ 98% and > 99.5% in experiments by Konczol *et al.* and Guichard *et al.*, respectively). Furthermore, both groups reported that the nanoparticles were mainly present as aggregates or agglomerates in cell culture media, and they were incorporated into the cells (Konczol *et al.*, 2011; Guichard *et al.*, 2012). Thus, further toxicity studies are required to increase our understanding of the toxic potential of magnetite nanoparticles.

The present study aims to examine the genotoxicity/clastogenicity of nanosized magnetite particles in cultured human and rodent cells using the *in vitro* MN test and sister chromatid exchange (SCE) test. We also assessed the phosphorylation of H2AX (γH2AX), a marker of DNA double strand breaks (DSB), and ROS production in cells treated with the particles.

MATERIALS AND METHODS

Nanomaterial

Magnetite nanoparticles with a primary particle size of 10 nm were purchased from Toda Kogyo Corp. (Hiroshima, Japan). Their specific surface area was 116 m²/g (disclosed by Toda Kogyo). The particles were suspended in water at a concentration of 2 mg/ml. For the cell treatments, the suspension was further diluted with saline (Otsuka Pharmaceutical Co. Ltd., Tokyo, Japan) containing 0.05% of Tween 80 (Nacalai Tesque, Kyoto, Japan) and then sonicated for 15-20 min.

Micronucleus test

The MN test was carried out as described previously (Totsuka *et al.*, 2009). Briefly, human lung carcinoma A549 cells and Chinese hamster ovary (CHO) AA8 cells obtained from the RIKEN Cell Bank (Wako, Japan) were cultured in Eagle's minimum essential medium (Nissui Pharmaceutical Co. Ltd., Tokyo, Japan) supplemented with 10% fetal bovine serum (JRH Biosciences, Lenexa, KS, USA) at 37°C in a 5% CO_2 atmosphere. The cells (A549, 7 × 10⁵ cells/dish; CHO AA8, 4 × 10⁵ cells/dish) were then seeded in plastic cell culture dishes (φ60 mm) one day before the treatment procedure. Suspensions of the nanoparticles were sonicated for 5-10 min at room temperature, and one volume of the suspension was mixed with 9 volumes of the culture medium supplemented with 10% fetal bovine serum (total: 3.3 ml/dish). Then, the cells were treated with the nanoparticles at the indicated concentrations for 6 hr. After being treated, the A549 and CHO AA8 cells were cultured for a further 42 or 20 hr, respectively. In the treatments involving anti-oxidants, the cells were cultured with medium containing the indicated concentration of *N*-acetylcysteine (NAC; Nacalai Tesque) or α-tocopherol (Nacalai Tesque) for 1 hr before the magnetite nanoparticle treatment. The cells were then treated with the nanoparticles for 6 hr, before being cultured for 42 hr (A549 cells) or 20 hr (CHO AA8 cells) in the presence of the anti-oxidants. Then, the cells were trypsinized, counted, and centrifuged. Growth inhibition was calculated using following the formula:

Growth rate = (the number of treated cells) ÷ (the number of non-treated cells)

The cells were then resuspended in 0.075 M KCl and incubated for 5 min, before being fixed 4 times in methanol:glacial acetic acid (3:1) and washed with methanol containing 1% acetic acid. Finally, the cells were resuspended in methanol containing 1% acetic acid. The cell solution was dropped onto slides, and then the nuclei were stained by mounting the cells with 40 μg/ml acridine orange (Nacalai Tesque) solution and immediately observed by fluorescence microscopy using blue excitation. The number of cells with MN was recorded based on the observation of 1,000 interphase cells.

Detection of γH2AX

To detect DSB, immunostaining of γH2AX was carried out as described previously (Shimohara *et al.*, 2008). Briefly, the A549 cells were seeded on glass slides at a density of 4 × 10⁵ cells/ml. The cells were then exposed to the nanoparticles for 1 hr as described above, but with serum-free medium, before being cultured for 1 hr with medium containing 10% fetal bovine serum. Etoposide (final concentration: 100 μg/ml; Sigma-Aldrich Japan, Tokyo, Japan) was used as a positive control. The cells were fixed on the glass slides with methanol, rinsed with ice-cold PBS (Takara Bio Inc., Shiga, Japan), and immersed in PBS containing 5% Triton X100 (ICN Biomedicals Inc., Irvine, CA, USA) for 30 min. The cells were then rinsed with ice-cold PBS and kept in PBS containing 5% bovine serum albumin (Sigma-Aldrich Japan) for 18 hr at room temperature, before being rinsed in PBS and treated with an anti-phospho-H2AX mouse